Ultraviolet-ozone irradiation of HPMC thin films: Structural and thermal properties

Nabawia A. Abdel-Zaher[1], Manal T.H. Moselhey[2] and Osiris W. Guirguis[*3]

[1]Textile Metrology Lab, National Institute for Standards, Giza, Egypt
[2]Al-Safwa High Institute of Engineering, Cairo, Egypt
[3]Department of Biophysics, Faculty of Science, Cairo University, Giza, Egypt

Abstract. The aim of the work was to evaluate the effect of ultraviolet-ozone (UV-O$_3$) irradiation with different times on the structure and thermal properties of hydroxypropyl methylcellulose (HPMC) in the form of a thin film to be used as bioequivalent materials according to their important broad practical and medical applications. HPMC thin films were exposed to UV-O$_3$ radiation in air at a wavelength of 184.9 nm.The beneficial effects of this treatment on the crystallinity and amorphousity regions were followed by X-ray diffraction technique and FTIR spectroscopy. Differential scanning calorimetry, thermogravimetric and differntial thermal analyses were used in order to study the thermal properties of HPMC samples following the process of photodegradation. The obtained results indicated that the rate of degradation process was increased with increasing the exposure time. Variations in shape and area of the thermal peaks were observed which may be attributed to the different degrees of crystallinity after exposing the treated HPMC samples. This meant a change in the amorphousity of the treated samples, the oxidation of its chemical linkages on its surface and its bulk, and the formation of free radical species as well as bond formation.

Keywords: HPMC; photodegradation; X-ray diffraction; FTIR spectroscopy; thermal properties

1. Introduction

Hydroxypropyl methylcellulose (HPMC) belongs to group of cellulose ethers, non-toxic and has hydrophilic nature (Hofenk-de Graaff 1981). HPMC has been used for a year by paper of conservators as glue, sizing and adhesives (Paradossi *et al.* 2003). According to the versatile properties of HPMC biopolymer, many applications in the food, cosmetic, and pharmaceutical industries were found. HPMC was used in the hydrogel technology and has emerged as a good substitute as a coating/film for drug delivery due to its hydrophilic nature (Siepmann and Peppas 2008, Ferrero *et al.* 2010, Gendre *et al.* 2011, Ku *et al.* 2011, Maderuelo *et al.* 2011, Yinghui Wei *et al.* 2012).

Due to the ability of HPMC to form a colloidal solution, it was also used as a drug carrier, and as an emulsifier for pharmaceutical creams as well as cosmetic lotions. It was used in hair care,

---

∗Corresponding author, Ph.D., E-mail: osiris_wgr@yahoo.com

skin care serums, shaving products, sun care products, and personal care formulations (METHOCEL Cellulose Ethers, Technical Handbook 2002). Due to its water retention behavior, HPMC was common used in eye medication and as a lubricant in the formulation of eye drop, other ophthalmologic aids and relieves dryness and irritation in the cornea of the eye (Schulz and Daniels 2000). On other hand, for industrial applications such as in the construction industry, HPMC was used as an adhesive and as an agent to mitigate the presence of water. Also, HPMC was effective in changing the texture of whipped cream (Zhao *et al.* 2009).

The effect of different exposure times on HPMC was reported by following X-ray diffraction analyses, infrared spectroscopy and thermal studies. These methods were capable of following small and rapid changes in the crystalline structure arising from ionizing radiation such as gamma-rays (Abd El-Kader *et al.* 2008).

Energy radiations, such as ozone change the physical and chemical properties of the materials they pass through. They generate free and trapped radicals, a displacement of orbital electrons and possibly atoms from their sites in the polymer matrix and a change in the number and nature of bonds, resulting in the formation of color centers (Lim *et al.* 1990). Organic molecules interact with UV light giving rise to various reactive species such as free radicals, excited molecules, and ions that react with atomic oxygen to form highly oxygenated carbons and volatile molecules. Also, UV light has the ability to depolymerize a variety of thin films photoresist polymers (Bolon and Kunz 1972). Moreover, exposure of film's surface to ozone (O_3) raised the surface oxidization and a consequence of O_3 formation-decomposition combined reactions were occurred which was also carried out with UV irradiation. After ozone treatment, degradation phenomenon may arise. By adjusting the exposure time, this phenomenon can be controlled. UV-O_3 treatment was efficient in terms of sealing and modification of polymers. Significant modification of the film surface composition was resulted by using UV-O_3 for a short treatment time. On other side, longer treatment time indicated further increase in oxygen concentration (Le *et al.* 2004). In conclusion, the oxygen concentration reaches a saturated value by increasing the UV-O_3 exposure time.

In the present work, the effect of UV-O_3 irradiation with different times on the structure and thermal properties of HPMC in the form of a thin film were investigated. In this approach, the crystallinity and amorphousity regions were followed by X-ray diffraction technique and FTIR spectroscopy. In order to study the thermal properties following the process of photodegradation, differential scanning calorimetry and thermogravimetric analyses were used.

2. Materials and methods

2.1 Materials and sample preparation

Hydroxypropyl methylcellulose (HPMC; Pharmacoat 606) with MW 133400 g/mol was supplied from Shin Etsu Chemical Co., Japan.

To prepare thin transparent films of HPMC the solution-cast method was used (El-Zaher and Osiris 2005, Abdel-Zaher *et al.* 2016). Pure HPMC solution was formed using weighted amount of HPMC in the form of a white powder and added in small increments to double distilled water. To promote complete dissolution, the solution was mixed lightly with a magnetic stirrer for about 2 h at 50°C while carefully controlling any increase in temperature above 50°C. High agitation was avoided since this could lead to the formation of air bubbles and foam in the solution, which were hard to remove. After 30 minutes the heat was removed, and the pure HPMC solution was cast

onto stainless steel Petri dishes (10 cm in diameter) and kept at room temperature (≈25°C) for 7 days until the water completely evaporated. Finally, thin transparent HPMC films of about 0.01 cm in thickness were formed and then kept in desiccators containing fused calcium chloride to avoid moisture.

The prepared HPMC thin films are exposed to UV-O$_3$ with different exposure times (1, 2, 3 and 4 h). High intensity, low-pressure mercury lamp without outer envelope -LRF 02971, 200 watt, 220 volt (Poland) placed in a cubic box with side length 60 cm was used as the UV-O$_3$ source at National Institute for Standards, Giza, Egypt. Atomic oxygen is generated both when molecular oxygen is subjected to the 184.9 nm radiation and when ozone was irradiated at 253.7 nm. The 253.7 nm radiation was absorbed by most hydrocarbons and also by ozone (Michael *et al.* 2004, Smith 2011, Abdel-Zaher *et al.* 2016). The samples of dimensions 1×4 cm were placed around the source at a distance 20 cm.

2.2 Characterizations of the prepared HPMC films

2.2.1 X-ray diffraction (XRD)

The XRD of HPMC films was measured by using a Phillips PW1840 X-Ray Diffractometer (USA) with an anode tube of CuK$_\alpha$ radiation (λ=1.54056 Å), operated at 40 kV and 25 mA. The patterns were recorded in the range of 2θ from 5 to 90° at a speed rate of 2 degrees/minute. The crystallinity index (CrI) (i.e., the time-save empirical measure of relative crystallinity) of the sample was calculated using the relation (Segal *et al.* 1959)

$$CrI=[(I_f - I_s)/I_f]\times100 \tag{1}$$

Where I_f is the peak intensity of the fundamental band and I_s is the peak intensity of the secondary band.

2.2.2 Fourier transform infrared (FTIR) spectroscopy

The absorption spectra of the prepared HPMC films over the range 4000-500 cm^{-1} were performed by using Fourier transform infrared (FTIR) Spectrophotometer, model Bruker Vector 22 (Germany) with accuracy better than ±1%.

2.2.3 Thermal analyses

The thermal properties of the prepared HPMC films were analyzed by using Differential Scanning Calorimetry (DSC) model Schimadzu DSC-50 (Kyoto, Japan) and Thermogravimetric Analyzer model Schimadzu TGA-50H (Kyoto, Japan). The DSC, TGA and DTA analyses cover the range from 25 to 650°C were performed under nitrogen atmosphere of rate of flow 20 mL/minute and at rate of heating of 10°C/minute. The average weight of the sample was about 6 mg. The standard uncertainty of the sample weight measurement was ±1% and the instrument was calibrated using calcium oxalate.

3. Results and discussion

3.1 X-ray diffraction analysis

The XRD patterns of unexposed and UV-O$_3$ exposed HPMC films were shown in Fig. 1. The pattern of unexposed HPMC sample showed amorphous features characterized by two different

Table 1 Variations in the values crystallinity index (CrI) and their percentage changes for unexposed and exposed HPMC films

HPMC samples UV-O$_3$ exposure times (h)	Crystallinity index (CrI)	Δ(CrI) % [*]
Unexposed	46.667	-
1	14.289	69.4
2	13.333	71.4
3	14.286	69.4
4	15.385	67.0

[*] $\Delta(\text{CrI})\% = \dfrac{(\text{CrI})_{\text{Unexposed}} - (\text{CrI})_{\text{Exposed}}}{(\text{CrI})_{\text{Unexposed}}} \times 100$

halos centred at 2θ=9.82 and 19.50° and one peak at about 13.5° which corresponding to semi-crystalline nature of HPMC. This result was in agreement with that previously reported by Sakata et al. ($2\theta\approx$10 and 20°) (Yukoh Sakata *et al.* 2006). It is also clear from the figure for the exposed XRD patterns that, the two distinguished peak were shifted toward higher values of 2θ by about 5 to 6° which may be attributed that during exposure the energy dissipated in the HPMC polymeric network caused chain scission or produced radicals which subsequently decayed with neighbouring radicals. In addition, the intensity of the first halo which represented the fundamental band (around 19 to 20°) decreased by increasing the time of exposure while the intensity of the second halo (secondary band, around 9 to 10°) increased as the exposure time increases. These variations meant that crystallinity of HPMC decreased. The peak at $2\theta\approx$13.5° was disappeared with increasing the exposure time up to 3 h. Two peaks were observed at $2\theta\approx$14.0 and 16.8° when the HPMC film exposed to UV-O$_3$ for 4 h which meant that increase in crystalline form was represented.

The development of crystallinity in a polymer was dependent upon its structural regularity and the factors that affected this crystallinity include: polarity, presence of hydrogen links as well as the ability to peak polymer chain (Madhu Mohan *et al.* 2005). XRD was used to measure the degree of crystallinity in polymers. As shown from the XRD patterns in Fig. 1, two distinguish bands were detected and centred in the ranges 2θ=19.50°-19.90° as fundamental band and 2θ=9.00°-9.82° as a secondary one. Table 1 represents the variation of crystallinity index (CrI) with UV-O$_3$ exposure time as calculated from the XRD patterns.

It was clear from the table that, maximum value of crystallinity index was detected for unexposed HPMC sample and decreased sharply with increasing the exposure time up to 3 h, and then the value of CrI increased again by increasing the exposure time to 4 h. This decrease in the value of CrI means that there was an increase in the amorphousity of HPMC network (i.e., decrease in crystallinity) due to UV-O$_3$ exposure and suggested the dominant presence of amorphous phase (Sakellariou *et al.* 1993).

From the obtained XRD and CrI results, it has been recognized that the exposure time plays a dominant role in both morphological and microstructural change in the polymer matrix (Abd El-Kader *et al.* 2008). This may be attributed to variation in the internal mechanisms that occurred by
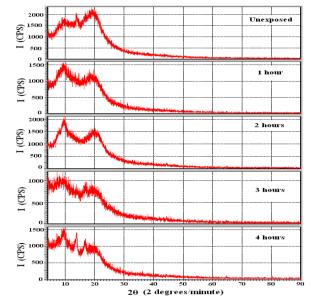
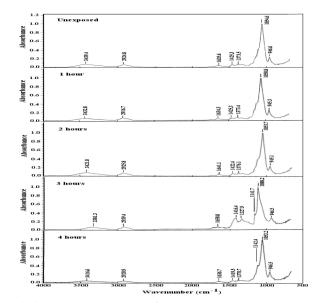Fig. 1 XRD patterns of unexposed and exposed HPMC films

Fig. 2 Variations in FTIR spectra of unexposed and exposed HPMC films

the induced effect of exposure time on the structure of HPMC (El-Zaher and Osiris 2005).

3.2 FTIR spectral analyses

The FTIR absorbance spectra of HPMC samples as functions of wavenumber in the range 4000-500 cm^{-1} were shown in Fig. 2. The chemical assignments were considered and were illustrated in Table 2.

Table 2 Positions and assignments of the most absorption bands of unexposed and exposed HPMC films

	Wavenumber (cm^{-1})				Assignments
Unexposed	UV-O$_3$ exposure times (h)				
	1	2	3	4	
3439.4	3432.8	3421.0	3381.3	3416.6	Hydrogen bonded and hydroxyl O-H group
2924.8	2916.7	2925.8	2939.4	2920.9	Symmetrical stretching modes of C-H bonding in the methyl group (CH$_2$ or CH$_3$ stretching vibration)
2907.0	2906.2	2907.6	2910.3	2907.4	C-H stretching vibration
1635.6	1634.3	1641.1	1658.8	1636.4	Water absorption and C=O stretching ester group
1425.3	1425.3	1422.4	1416.4	1419.5	O-H, C-H bending and CH$_2$ deformation
1373.5	1373.4	1376.1	1327.9	1370.7	Associated with C-O stretching vibration and -CH$_2$ wagging
1141.3	1140.8	1141.4	1141.7	1142.4	Asymmetric stretching vibration of C-C groups and symmetric C-O stretching vibration
1054.6	1050.8	1053.7	1088.2	1053.2	C-O stretching vibration
946.6	945.3	945.1	946.5	946.5	C-O deformation and CH$_2$ rocking

From the figure and the table, it was noticed that the FTIR spectrum of unexposed HPMC indicated the details of functional groups present in correlation with previous investigations (Desai and Shields 1969, Smith 1979, Kim *et al.* 1992, Sakellariou *et al.* 1993, Park *et al.* 1995, Bernard *et al.* 2003, Osiris and Manal 2011). It was clear from the figure and the table for unexposed HPMC sample that a relatively broad and intense OH absorption stretching band was observed at about 3439 cm^{-1} which may be due to the free hydroxyl group and hydrogen bonded OH stretching vibration. Distinct absorption bands were occurred at about 2925 and 2907 cm^{-1} result from the antisymmetric stretching band of CH$_2$ or CH$_3$ group. No significant absorption until about 1640 cm^{-1} was detected. The band at about 1636 cm^{-1} may be due to C=O stretching mode appears. The symmetric bending mode (CH$_2$) was found at about 1425 cm^{-1}. The band at 1374 cm^{-1} was associated with C-O stretching vibration and wagging vibration of CH$_2$. The relatively intense band at about 1141 cm^{-1} was related to the asymmetric stretching vibration of C-C group and symmetric C-O stretching vibration. In addition, it was inferred that the 1141 cm^{-1} band might be due to a kind of absorption mechanism related to the presence of the oxygen atom. The band at about 1055 cm^{-1} was assigned to C-O stretching vibration of ether group. Finally, the band at about 947 cm^{-1} was assigned to the C-O deformation and CH$_2$ rocking vibration.

The FTIR spectra of the most evident absorption bands for UV-O$_3$ exposed HPMC samples were also represented in Fig. 2 and Table 2. It was noticed that, decrease of broadness band and its intensity at about 3417 cm^{-1} (4 h HPMC sample) was detected. Also there were changes in the band positions and intensities of the other bands by increasing the time exposure to UV-O$_3$ allowed us to specify a strong or weak interaction between HPMC ions. The position and the bonding of these groups were influenced by crystallinity and crystal modification. The increase in absorbance of carbonyl groups indicates decrease in their growth and may suggest that they were converted into volatile compounds (Smith 1979). The observed change in intensity of some spectra of exposed HPMC may be attributed to the fact that the resulting spectrum was approximately the sum of two or more components. On other hand, the type of bonding in the network structure may

Table 3 Values of transition temperatures and associated heat of fusion for unexposed and exposed HPMC films

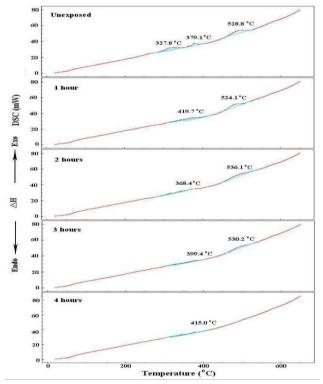| HPMC films	At melting transition region			
	First step		Second step	
UV-O$_3$ exposure times (h)	T_m (^{o}C)	ΔH_m (J/g)	T_m (^{o}C)	ΔH_m (J/g)
Unexposed	327.8	78.76	528.8	139.17
	379.1	49.01		
1	419.7	50.22	524.1	128.66
2	368.4	36.21	536.1	118.03
3	399.4	34.04	530.2	76.97
4	415.0	-9.05	Not detected	

Fig. 3 DSC curves for unexposed and exposed HPMC films

play a dominant role in deciding the rigidity of the structure and also associated with the change in degradation and/or cross-linkage and coordination of the polymer network (Bernard *et al.* 2003, Osiris and Manal 2011).

3.3 Thermal analyses

3.3.1 Differential scanning calorimetry (DSC)
The glass transition temperature, crystallization temperature, heat of crystallization, melting
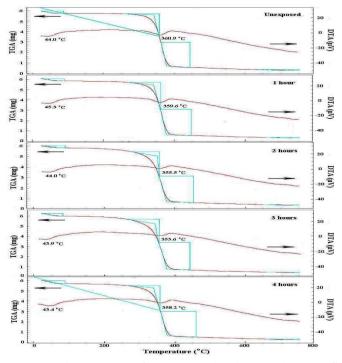
Fig. 4 TGA and DTA curves for unexposed and exposed HPMC films

Table 4 TGA data for unexposed and exposed HPMC films

HPMC films	At First order thermodynamic transition region (First step)		At melting transition region					
			Second step		Third step		Fourth step	
UV-O_3 exposure times (h)	% weight loss	Mid point (^{o}C)	% weight loss	Mid point (^{o}C)	% weight loss	Mid point (^{o}C)	% weight loss	Mid point (^{o}C)
Unexposed	3.450	43.96	34.718	346.72	40.529	370.94	1.340	677.82
1	3.721	45.30	44.113	348.51	41.874	370.35	0.840	693.43
2	3.464	43.99	41.223	341.33	41.471	367.26	0.945	694.24
3	4.228	43.87	39.062	336.73	43.147	366.00	0.967	701.00
4	5.199	43.38	40.193	343.01	41.226	368.49	1.100	685.12

temperature, heat of fusion and degree of crystallinity were the basis thermal parameters and can be determined by DSC curves. Fig. 3 shows the DSC curve of unexposed HPMC sample and curves after being exposed to different times of irradiation (1, 2, 3 and 4 h) in the range of temperature from 25°C up to 650°C. It is clear from the figure that, the DSC thermogram of the unexposed HPMC sample showed three exothermic stages while exposed samples showed two broad exothermic stages except the 4 h exposed sample which showed one single exothermic stage. It was also noticed that, differences in shape and area of the melting exotherms were observed. The variations in shape and area were attributed to the different degrees of crystallinity

Table 5 The total % weight loss and the residue % of unexposed and exposed HPMC films

HPMC films UV-O$_3$ exposure times (h)	Total % weight loss	Residue %
Unexposed	80.037	19.963
1	90.548	9.452
2	87.103	12.897
3	87.404	12.596
4	87.718	12.282

found in the samples with different exposure times.

Table 3 depicts the melting transition temperatures and the heat of fusion (ΔH_m) of each transition obtained through the analysis of DSC curves for both unexposed HPMC sample as well as of samples after different times of UV-O$_3$ exposure. It was clear from the table that, two melting transition temperatures were detected except the 4 h exposed sample which showed one single value. In addition, while the time of irradiation increases, the values of melting temperatures of exposure HPMC samples increase and the values of heat of fusion decrease. As reported in literatures that, melting of polymers was depended on the degree of crystallinity, ordering of macromolecules and molecular weight of the polymer (Bras *et al.* 2007). In the DSC curves of HPMC samples, two melting transition temperatures were detected. This observation can be explained by coexistence of more than one degradation process of melting which was typical of bimodal polymers (Song *et al.* 2013). Moreover, a change in the crystalline structure could be due to polymer interactions in the amorphous phase, and then disorder in the crystals was created reducing the enthalpy of the phase change (Hammel *et al.* 1975).

3.3.2 Thermogravimetric (TGA) and differential thermal (DTA) analyses

Thermal degradation behaviors of unexposed and exposed HPMC were examined by thermogravimetric analyses (TGA) as shown in Fig. 4. In addition, the difference in thermal decomposition behaviors of the unexposed and exposed HPMC samples can also be seen from the differential thermal analyses (DTA) curves (Fig. 4). It is clear from the figure for both TGA and DTA analyses that, the degradation behaviors of the photodegradation of HPMC samples were almost similar to the behavior of the unexposed one. Two decomposition stages were recorded for both unexposed and exposed HPMC samples which suggested the coexistence of more than one degradation process. In addition, a reduction of HPMC sample decomposition temperatures along with the increase in photodegradation time.

Table 4 depicts the TGA data for unexposed and exposed HPMC films with UV-O$_3$ for different exposure times. It was noticed from the table for the unexposed and exposed HPMC samples that the first decomposition stage (i.e., at the first order thermodynamic transition region) showed lower values of % weight loss (3.450-5.199). More significant values of % weight loss (76.587-82.519) were detected for the second decomposition stage (i.e., at the melting transition region). Before UV radiation the first decomposition temperature of HPMC sample equaled about 44°C and non-remarkable decreased to about 43°C after 4 h of irradiation. The first decomposition temperature depends on the structure of the polymer chain, its elasticity and the molecular weight of the polymer (Ewa Olewnik-Kruszkowska 2015). The lower values of % weight loss in the first order thermodynamic transition region started at about 40°C confirm the presence of a thermal

process due to water loss or moisture evaporation from the samples and also may be due to splitting or volatilization of small molecules and/or monomers which may be explained by the existence of physical transition and also could be corresponded to the breaking of the ester linkages (Kim *et al.* 1992, Neto *et al.* 2005). The second decomposition stage (consisted of 3 steps) in TGA curves covered a wider temperature range (90-700°C), included the melting temperature points. This stage was corresponded to the weight loss due to the decomposition of the HPMC structure and was the most important stage both in the rate of % weight loss and in the total % weight loss. For unexposed HPMC sample, this second decomposition stage was characterized by the presence of the typical melting endotherms at about 347, 371 and 678°C. The difference in temperatures (ΔT) between the unexposed HPMC sample and the sample irradiated for 4 h for the three steps equaled about 5, 5, and 23°C, respectively. Thermal stability of the samples can be evaluated by these temperatures of the thermal decomposition stages, which is in agreement with that previously reported by Chiu (Chiu 1966). The higher values of % weight loss in this stage indicated the existence of a chemical degradation process resulting from cellulose ethers degradation of HPMC and also bond scission (carbon-carbon bonds) in the polymeric backbone and may have corresponded to the degradation of the whole polymer. It is noteworthy that thermostability of HPMC after photodegradation time up to 3 h increases indicated by the reduced ΔT values. In addition, upon heating HPMC above the decomposition temperature the polymer began a rapid chain-stripping elimination of H_2O (Cullis and Hirschler 1981).

Table 5 indicates the total % weight loss and the residue % of the unexposed and exposed HPMC films to UV-O_3 for different exposure times. It is noticed that, the total % weight loss values of the exposed HPMC samples were slightly lower than the value of the unexposed sample except for the HPMC sample exposed for 1 h which showed the highest value. On other hand, the char residue % (=100–Total % weight loss) for 1 h exposure sample had the lowest value than those of both the unexposed and other exposed samples. This indicated that the thermal stability of the samples was reduced and they are low resistant to fire hazards.

The differential thermal analysis (DTA) data represented in Fig. 4 indicated that the photodegradation process of HPMC was accelerated during exposure to UV radiation.

4. Conclusions

The present work deals with studying the effect of UV-O_3 as a source of physical treatment on improving the structural and thermal properties of prepared HPMC thin films. Exposure to UV-O_3 plays role in both morphological and micro-structural change in the polymer matrix. The obtained results indicated that structural changes occurred in HPMC network. The XRD study showed that the decrease in crystallinity index has been proposed as one or another aspect of the complicated molecular and crystalline structure induced when exposed with UV-O_3. The obtained FTIR data noticed that there was a variation in the band intensity values of the HPMC functional groups which may lead to better improvement in their chemical behavior. In addition, the DSC, TGA and DTA studies revealed the fundamental changes in the morphology of the HPMC and thermal stability.

It can be concluded that HPMC thin films exposed to UV-O_3 can have a wide range of industrial applications such as packing and coverage which depend on the knowledge of the physical and chemical properties of the materials used. Moreover, the use of biomaterials may reduce the use of non-renewable resource materials and reduce pollution levels.

References

Abd El-Kader, F.H., Gaafar, S.A., Mahmoud, K.H., Bannan, S.I. and Abd El-Kader, M.F.H. (2008), "γ-irradiation effects on the thermal and optical properties of undoped and eosin doped 70/30 (wt/wt%) PVA/glycogen films", *Curr. Appl. Phys.*, **8**(1), 78-87.

Bernard, C., Chaussedent, S., Monteil, A., Montagna, M., Zampedri, L. and Ferrari, M. (2003), "Simulation by molecular dynamics of erbium-activated silica-titania glasses", *J. Sol-Gel Sci. Technol.*, **26**(1), 925-929.

Bolon, D.A. and Kunz, C.O. (1972), "Ultraviolet depolymerization of photoresist polymers", *Polym. Eng. Sci.*, **12**(2), 109-111.

Bras, A.R., Viciosa, M.T., Dionisio, M. and Mano, J.F. (2007), "Water effect in the thermal and molecular dynamics behaviour of poly(l-lactic acid)", *J. Therm. Anal. Calorimet.*, **88**(2), 425-429.

Chiu, J. (1966), "Applications of thermogravimetry to the study of high polymers", *Appl. Polym. Symp.*, **2**, 25-43.

Cullis, C.F. and Hirschler, M.M. (1981), *Combustion of Organic Polymers*, Clarendon Press, Oxford, U.K.

Desai, R.L. and Shields, J.A. (1969), "Photochemical degradation of cellulose material", *Die Makromol. Chem.*, **122**(1), 134-144.

El-Zaher, N.A. and Osiris, W.G. (2005), "Thermal and structural properties of poly(vinyl alcohol) doped with hydroxypropyl cellulose", *J. Appl. Polym. Sci.*, **96**(5), 1914-1923.

Ewa, O.K. (2015), "Effect of UV irradiation on thermal properties of nanocomposites based on polylactide", *J. Therm. Anal. Calorimet.*, **119**(1), 219-228.

Ferrero, C., Massuelle, D. and Doelker, E. (2010), "Towards elucidation of the drug release mechanism from compressed hydrophilic matrices made of cellulose ethers: II. Evaluation of a possible swelling-controlled drug release mechanism using dimensionless analysis", *J. Control. Rel.*, **141**, 223-233.

Gendre, C., Boiret, M., Genty, M., Chaminade, P. and Pean, J.M. (2011), "Real time predictions of drug release and end point detection of a coating operation by in-line near infrared measurements", *J. Pharmac.*, **421**(2), 237-243.

Hammel, R., MacKnight, W.J. and Karasz, F.E. (1975), "Structure and properties of the system: Poly(2,6-di-methyl-phenylene oxide) isotactic polystyrene wide-angle x-ray studies", *J. Appl. Phys.*, **46**(10), 4199-4203.

Hofenk-de, G.J. (1981), *Central Research Laboratory for Objects of Art and Science*, Gabriel Metsustroat and 1071 EA, Amsterdam, the Netherlands.

Kim, J.H., Kim, J.Y., Lee, Y.M. and Kim, K.Y. (1992), "Properties and swelling characteristics of cross-linked poly(vinyl alcohol)/chitosan blend membrane", *J. Appl. Polym. Sci.*, **45**(10), 1711-1717.

Ku, M.S., Lu, Q., Li, W. and Chen, Y. (2011), "Performance qualification of a new hypromellose capsule: Part II. Disintegration and dissolution comparison between two types of hypromellose capsules", *J. Pharmac.*, **416**(1), 16-24.

Lim, S.L., Fane, A.G. and Fell, C.J.D. (1990), "Radiation-induced grafting of regenerated cellulose hollow-fiber membranes", *J. Appl. Polym. Sci.*, **41**(7-8), 1609-1616.

Maderuelo, C., Zarzuelo, A. and Lanao, J.M. (2011), "Critical factors in the release of drugs from sustained release hydrophilic matrices", *J. Control. Rel.*, **154**(1), 2-19.

Madhu Mohan, V., Raja, V., Sharma, A.K. and Narasimha Rao, V.V.R. (2005), "Ionic conductivity and discharge characteristics of solid-state battery based on novel polymer electrolyte (PEO+NaBiF$_4$)", *Mater. Chem. Phys.*, **94**(2), 177-181.

METHOCEL Cellulose Ethers (2002), *Technical Handbook*, Trademark of the Dow Chemical Company, U.S.A.

Michael, M.N., El-Zaher, N.A. and Ibrahim, S.F. (2004), "Investigation into surface modification of some polymeric fabrics by UV/ozone treatment", *Polym.-Plast. Technol. Eng.*, **43**(4), 1041-1052.

Nabawia, A., Abdel-Zaher, M.T.H. and Osiris, W.G. (2016), "Optical studies of hydroxypropyl methylcellulose thin films exposed to UV/ozone", *J. Sci. Eng. Res.*, **3**, 84-96.

Neto, C.G.T., Giacometti, J.A., Job, A.E., Ferreira, F.C., Fonseca, J.L.C. and Pereira, M.R. (2005), "Thermal analysis of chitosan based network", *Carbohyd. Polym.*, **62**(2), 97-103.

Osiris, W.G. and Manal, T.H.M. (2011), "Optical study of poly(vinyl alcohol)/hydroxypropyl methylcellulose blends", *J. Mater. Sci.*, **46**(17), 5775-5789.

Paradossi, G., Cavalieri, F., Chiessi, E., Spagnoli, C. and Cowman, M.K. (2003), "Poly(vinyl alcohol) as versatile biomaterial for potential biomedical applications", *J. Mater. Sci.: Mater. Medic.*, **14**(8), 687-691.

Park, C.K., Choi, M.J. and Lee, Y.M. (1995), "Chelate membrane from poly(vinyl alcohol)/poly(*N*-salicylidene allyl amine) blend. I: Synthesis and characterization of Co(II) chelate membrane", *Polym.*, **37**, 1507-1512.

Qiangzhong, Z., Mouming, Z., Jianrong, L., Bao, Y., Guowan, S., Chun, C. and Yueming, J. (2009), "Effect of hydroxypropyl methylcellulose on the textural and whipping properties of whipped cream", *Food Hydrocol.*, **23**(8), 2168-2173.

Quoc, T.L., Whelan, C.M., Struyf, H., Vanhaelemeersch, S., Azioune, A., Louette, P., Pireaux, J.J. and Maex, K. (2004), "Polymer dielectric treatment using ultraviolet-ozone: A photoelectron spectroscopy and ellipsometric porosimetry study", *J. Appl. Phys.*, **96**(7), 3807-3810.

Sakellariou, P., Hassan, A. and Rowe, R.C. (1993), "Phase separation and polymer interactions in aqueous poly(vinyl alcohol)/hydroxypropyl methylcellulose blends", *Polym.*, **34**(6), 1240-1248.

Schulz, M.B. and Daniels, R. (2000), "Hydroxypropyl methylcellulose (HPMC) as emulsifier for submicron emulsions: Influence of molecular weight and substitution type on the droplet size after high-pressure homogenization", *Eur. J. Pharmac. Biopharmac.*, **49**(3), 231-236.

Segal, L., Creely, J.J., Martin Jr, A.E. and Conrad, C.M. (1959), "An empirical method for estimating the degree of crystallinity of native cellulose using the x-ray diffractometer", *Text. Res. J.*, **29**(10), 786-794.

Siepmann, J. and Peppas, N.A. (2001), "Modeling of drug release from delivery systems based on hydroxypropyl methylcellulose (HPMC)", *Adv. Drug Del. Rev.*, **48**, 139-157.

Smith, A.L. (1979), *Applied Infrared Spectroscopy, Fundamentals Techniques and Analytical Problem-Solving*, Wiley, New York, U.S.A.

Smith, B.C. (2011), *Fundamentals of Fourier Transform Infrared Spectroscopy*, 2nd Edition, CRC Press, Boca Raton, London, New York, U.S.A.

Song, P., Chen, G., Wei, Z., Zhang, W. and Liang, J. (2013), "Calorimetric analysis of the multiple melting behavior of melt-crystallized poly(L-lactic acid) with a low optical purity", *J. Therm. Anal. Calorimet.*, **111**(2), 1507-1514.

Yinghui, W., Xiaoli, Y., Xiaoguang, S., Xuan, P., Qiang, B., Minchen, L., Manman, G. and Fanzhu, L. (2012), "Enhanced oral bioavailability of silybin by a supersaturatable self-emulsifying drug delivery system (S-SEDDS)", *Coll. Surf. A: Physicochem. Eng. Asp.*, **396**, 22-28.

Yukoh, S., Sumihiro, S. and Makoto, O. (2006), "A novel white film for pharmaceutical coating formed by interaction of calcium lactate pentahydrate with hydroxypropyl methylcellulose", *J. Pharmac.*, **317**(2), 120-126.

CC